

Submitted for publication in the Astrophysical Journal

## A Search for the Transit of HD 168443b: Improved Orbital Parameters and Photometry

Genady Pilyavsky<sup>1</sup>, Suvrath Mahadevan<sup>1,2</sup>, Stephen R. Kane<sup>3</sup>, Andrew W. Howard<sup>4,5</sup>, David R. Ciardi<sup>3</sup>, Chris de Pree<sup>6</sup>, Diana Dragomir<sup>3,7</sup>, Debra Fischer<sup>8</sup>, Gregory W. Henry<sup>9</sup>, Eric L. N. Jensen<sup>10</sup>, Gregory Laughlin<sup>11</sup>, Hannah Marlowe<sup>6</sup>, Markus Rabus<sup>12</sup>, Kaspar von Braun<sup>3</sup>, Jason T. Wright<sup>1,2</sup>, Xuesong X. Wang<sup>1</sup>

`gcp5017@psu.edu`

`suvrath@astro.psu.edu`

### ABSTRACT

The discovery of transiting planets around bright stars holds the potential to greatly enhance our understanding of planetary atmospheres. In this work

---

<sup>1</sup>Department of Astronomy and Astrophysics, Pennsylvania State University, 525 Davey Laboratory, University Park, PA 16802

<sup>2</sup>Center for Exoplanets & Habitable Worlds, Pennsylvania State University, 525 Davey Laboratory, University Park, PA 16802

<sup>3</sup>NASA Exoplanet Science Institute, Caltech, MS 100-22, 770 South Wilson Avenue, Pasadena, CA 91125

<sup>4</sup>Department of Astronomy, University of California, Berkeley, CA 94720

<sup>5</sup>Space Sciences Laboratory, University of California, Berkeley, CA 94720

<sup>6</sup>Department of Physics and Astronomy, Agnes Scott College, 141 East College Avenue, Decatur, GA 30030, USA

<sup>7</sup>Department of Physics & Astronomy, University of British Columbia, Vancouver, BC V6T1Z1, Canada

<sup>8</sup>Department of Astronomy, Yale University, New Haven, CT 06511

<sup>9</sup>Center of Excellence in Information Systems, Tennessee State University, 3500 John A. Merritt Blvd., Box 9501, Nashville, TN 37209

<sup>10</sup>Dept of Physics & Astronomy, Swarthmore College, Swarthmore, PA 19081

<sup>11</sup>UCO/Lick Observatory, University of California, Santa Cruz, CA 95064

<sup>12</sup>Departamento de Astronomía y Astrofísica, Pontificia Universidad Católica de Chile, Casilla 306, Santiago 22, Chile

we present the search for transits of HD168443b, a massive planet orbiting the bright star HD 168443 ( $V = 6.92$ ) with a period of 58.11 days. The high eccentricity of the planetary orbit ( $e = 0.53$ ) significantly enhances the a-priori transit probability beyond that expected for a circular orbit, making HD 168443 a candidate for our ongoing Transit Ephemeris Refinement and Monitoring Survey (TERMS). Using additional radial velocities from Keck-HIRES, we refined the orbital parameters of this multi-planet system and derived a new transit ephemeris for HD168443b. The reduced uncertainties in the transit window make a photometric transit search practicable. Photometric observations acquired during predicted transit windows were obtained on three nights. CTIO 1.0 m photometry acquired on 2010 September 7 had the required precision to detect a transit but fell just outside of our final transit window. Nightly photometry from the T8 0.8 m Automated Photometric Telescope (APT) at Fairborn Observatory, acquired over a span of 109 nights, demonstrates that HD 168443 is constant on a time scale of weeks. Higher-cadence photometry on 2011 April 28 and June 25 shows no evidence of a transit. We are able to rule out a non-grazing transit of HD168443b.

*Subject headings:* planetary systems – techniques: photometric – techniques: radial velocities – stars: individual (HD 168443)

## 1. Introduction

The number of known exoplanets has grown rapidly in the last decade, with over 600 confirmed exoplanets known to date<sup>1</sup>. While most of these planets have been discovered using radial velocity techniques, the number of known transiting planets has increased significantly due to dedicated transit surveys like the space-based Kepler (Borucki et al. 2011) and CoRoT (Barge et al. 2008) missions, and ground-based transit searches like the Hungarian Automated Telescope Network (HATNet) (Bakos et al. 2004), SuperWASP (Pollacco et al. 2006), and XO (McCullough et al. 2005). The price for efficient operation of these wide-field transit surveys, though, is that most of the candidate stars tend to be fainter than those being surveyed by radial velocity. Of the over one hundred transiting planet host stars known, the sample of bright stars ( $V < 9$ ) with transiting planets is still limited to only nine stars: HD209458 (Charbonneau et al. 2000; Henry et al. 2000), HD189733 (Bouchy et al. 2005), HD149026 (Sato et al. 2005), HD17156 (Barbieri et al. 2007), HD80606

---

<sup>1</sup>exoplanet.eu

(Moutou et al. 2009; Fossey et al. 2009), HD97658 (Henry et al. 2011) and 55 Cnc e (Winn et al. 2011) (all of which were discovered by radial velocity surveys), while WASP-33b and HAT-P-2b were discovered by transit surveys and confirmed by radial velocity followup.

The discovery of additional bright transiting planet hosts is advantageous in further enabling studies of the atmospheric constituents of exoplanets. Even with the largest ground-based telescopes, transmission spectroscopy to probe the atmospheres of these exoplanets has, largely, been accomplished only for the brightest targets. Using high-resolution spectroscopy on 8–10 m telescopes, Redfield et al. (2008) and Snellen et al. (2008) detected sodium absorption in the transmission spectra of HD189733b and HD209458b, respectively. More recently, using the narrowband tunable filter imager on the 10 m GTC, Colon et al. (2010) and Sing et al. (2011) have detected the signature of potassium absorption in the atmospheres of HD 80606b and XO-2b.

Our ongoing Transit Ephemeris Refinement and Monitoring Survey (TERMS, Kane et al. (2009)) project focuses on bright stars ( $V < 9$ ) with known exoplanets and orbital periods greater than 10 days in an effort to refine the orbital parameters with additional radial velocity observations and then observe the targets photometrically within their revised transit windows. Transits detected around such bright stars would provide perfect candidates for spectroscopic follow up. In addition, with periods greater than ten days, the planet population searched by TERMS is not easily duplicable by ongoing ground-based transit surveys as demonstrated by von Braun et al (2009). In Kane et al. (2011) we presented the ephemeris revision and the search for a transit around HD 156846. In this paper, we present additional radial velocities and refine the transit ephemeris for the bright star HD 168443, which is known to have multiple companions. We present new photometry that allows us to rule out transits of HD 168443b.

## 2. HD 168443

HD 168443 (GJ 4052, HIP 89844, TYC 5681-1576-1) is a bright ( $V = 6.92$ ) G5 dwarf known to possess two substellar companions, forming a dynamically active system (Veras & Armitage 2007). HD 168443b (Marcy et al. 1999; Wright et al. 2009) has a reported  $M_p \sin i = 7.8 \pm 0.259 M_{Jup}$ , an orbit with a period of 58.11 days and a large eccentricity of  $e = 0.53$ . HD 168443c, a brown dwarf companion (Udry et al. 2002; Wright et al. 2009), has  $M_p \sin i = 17.5 \pm 0.65 M_{Jup}$ , an orbital period of  $\sim 1748$  days and a moderate eccentricity  $e = 0.21$ . Using the van Leeuwen (2007) re-reduction of the *Hipparcos* data, Reffert & Quirrenbach (2011) derive a mass of  $30.3^{+9.4}_{-12.2} M_{Jup}$  and a  $3\sigma$  upper mass limit of  $65 M_{Jup}$ , confirming that this object is indeed substellar. The  $3\sigma$  lower limit does not exclude an inclination of

90°, so the minimum mass derived from the radial velocities applies. From CORALIE radial velocities and the van Leeuwen (2007) *Hipparcos* re-reductions, Sahlmann et al. (2011) concluded that, while their formal solution for the mass of HD 168443c matched that of Reffert & Quirrenbach (2006), the mass was of "low confidence." They are unable to set an upper mass limit because the radial velocity orbit is not fully covered by their CORALIE observations. Dynamical simulations by Veras & Ford (2010) show that almost no stable systems can exist for mutual inclinations between HD 168443b and c of 60°–120°.

The eccentric orbit of HD 168443b increases its transit probability significantly above what one would expect for a planet in a circular orbit with the same period. The new orbital parameters, along with the formalism outlined in Kane et al. (2009), result in a transit probability of 3.7% compared to 2.5% for a circular orbit. While the atmospheric scale heights for massive, relatively cold planets are expected to be small (Vidal-Madjar et al. 2011), the brightness of HD 168443 (more than twice as bright as HD 209458, the third brightest star known to have a transiting planet) makes such detections possible with large ground-based telescopes.

The discovery of transits of the inner planet would also constrain the possible inclinations of the outer brown dwarf companion, enabling additional dynamical investigations. The predicted transit probability of 3.7%, coupled with the fact that HD 168443 is a very bright star, makes it an intriguing target in our ongoing attempts to discover long-period transiting planets.

### 3. Stellar Properties

We used Spectroscopy Made Easy (SME; Valenti & Piskunov 1996) to fit high-resolution Keck-HIRES spectra of HD 168443, applying the wavelength intervals, line data, and methodology of Valenti & Fischer (2005). We further constrained the surface gravity using Yonsei-Yale ( $Y^2$ ) stellar structure models (Demarque et al. 2004) and revised *Hipparcos* parallaxes (van Leeuwen 2007), with the iterative method of Valenti et al. (2009). The resulting stellar parameters listed in Table 1 are effective temperature, surface gravity, iron abundance, projected rotational velocity, mass, and radius. HD 168443 lies 1.05 mag above the *Hipparcos* average main sequence ( $M_V$  versus  $B - V$ ) as defined by Wright (2005). These properties are consistent with an evolved metal-rich G5 star. The stellar radius,  $R_\star = 1.51 \pm 0.06 R_\odot$ , is crucial for estimating the depth and duration of a planetary transit. This value is consistent with the interferometrically measured  $R_\star = 1.58 \pm 0.06 R_\odot$  (van Belle & von Braun 2009).

In addition, we computed the level of stellar activity in HD 168443 from the strength of

the Ca II H & K lines, which give calibrated  $S_{\text{HK}}$  values on the Mt. Wilson scale and  $\log R'_{\text{HK}}$  values (Isaacson & Fischer 2010). The median of  $\log R'_{\text{HK}}$  and  $S_{\text{HK}}$  values are listed in Table 1 and demonstrate that HD 168443 is chromospherically quiet. Additional examination of the available history of Ca II H & K measurements show no significant long-term variation in  $S_{\text{HK}}$ .

## 4. Keck-HIRES RV Measurements and Revised Orbital Model

### 4.1. Measurements

We observed HD 168443 using the standard procedures of the California Planet Search (CPS) for the HIRES echelle spectrometer (Vogt et al. 1994) on the 10 m Keck I telescope. These measurements span fifteen years, 1996 July to 2011 March, and comprise one of the longest RV datasets presented for a star with one or more known planets. The initial measurements in this time series were used to discover the two planets (Marcy et al. 1999, 2001) while later measurements refined the orbits (Wright et al. 2009). The full set of measurements presented here refines the orbit further and gives an accurate predicted transit ephemeris with which we search for photometric transits.

The 130 Keck RV measurements (Table 2) were made from observations with an iodine cell mounted directly in front of the spectrometer entrance slit. The dense set of molecular absorption lines imprinted on the stellar spectra provide a robust wavelength fiducial against which Doppler shifts are measured, as well as strong constraints on the shape of the spectrometer instrumental profile at the time of each observation (Marcy & Butler 1992; Valenti et al. 1995). We measured the Doppler shift of each star-times-iodine spectrum using a modeling procedure descended from Butler et al. (1996) as described in Howard et al. (2009). The times of observation (in barycentric Julian days), relative RVs, and associated errors (excluding jitter) are listed in Table 2. We also observed HD 168443 with the iodine cell removed to construct a stellar template spectrum for Doppler modelling and to derive stellar properties.

### 4.2. Keplerian Model

We modelled the Keck RVs as the superposition of the Keplerian interactions from two planets with the star, plus a linear trend in velocity due to a distant and massive third companion. We used the orbit fitting techniques described in Howard et al. (2010) and the

partially linearized, least-squares fitting procedure described in Wright & Howard (2009). Each velocity measurement was assigned a weight,  $w$ , constructed from the quadrature sum of the measurement uncertainty ( $\sigma_{\text{RV}}$ ) and a jitter term ( $\sigma_{\text{jitter}}$ ), i.e.,  $w = 1/(\sigma_{\text{RV}}^2 + \sigma_{\text{jitter}}^2)$ . We chose jitter values of  $\sigma_{\text{jitter}} = 3$  and  $2 \text{ m s}^{-1}$  for measurements before and after the HIRES upgrade in August 2004. These values are consistent with the expected jitter of a slightly evolved early G star observed with Keck/HIRES Wright (2005). Possible sources of jitter include stellar pulsation, magnetic cycles, granulation, undetected planets, and instrumental effects (Isaacson & Fischer 2010; Wright 2005).

Our best-fit orbital model is presented in Table 3 and Figure 1. The Keplerian parameter uncertainties for each planet were derived using a Monte Carlo method (Marcy et al. 2005) and account for correlations between parameter errors. Uncertainties in  $M \sin i$  and  $a$  reflect uncertainties in  $M_*$  and the orbital parameters. We considered and rejected more complicated models having a third planet and/or a quadratic velocity trend because of statistically insignificant changes in  $\chi^2$  compared to the adopted model (Table 3).

## 5. Transit Ephemeris Refinement

The revised orbital solution presented in Table 3 for this multi-planet system, along with the stellar properties in Table 1, allow us to construct an accurate transit ephemeris from which to conduct a search for transits. As shown by Kane & von Braun (2008), the transit probability of a planet is intricately related to both the orbital eccentricity and the argument of periastron. Figure 2 depicts the orbits of the planets relative to the observer line-of-sight and shows how the eccentricities and orientations affects the star-planet separation along that line.

We use the models of Bodenheimer et al. (2003) to estimate a radius for HD 168443b of  $R_p = 1.11 R_{\text{Jup}}$ , which takes into account orbital parameters and the stellar flux received by the planet. This results in a transit probability of 3.7% and a predicted transit depth of 0.6%. The predicted transit duration is 0.36 days, or 8 hours and 40 minutes. The time of mid transit shown in Table 3 is for 2011 March 1. The calculation was performed using a Monte-Carlo bootstrap which propagates the uncertainties in the orbital parameters forward to the time of transit. The uncertainty in this predicted time is small; only  $\sim 35$  minutes. Thus, the predicted duration of the transit window for this date is 9 hours and 50 minutes (the sum of the predicted duration  $\pm 1\sigma$  deviation), overwhelmingly dominated by the predicted transit duration rather than the uncertainty associated with the orbital parameters. The predicted duration makes complete coverage of the transit window from a single ground-based longitude difficult, though the predicted depth is sufficient to rule out

transits from observations during times of ingress or egress only.

## 6. *Hipparcos* Photometry of HD 168443

The *Hipparcos* mission observed the brightest stars in the sky over many epochs. Robichon & Arenou (2000) and Castellano et al. (2000) detected the transit of HD 209458b in the *Hipparcos* epoch photometry, and Hébrard & Lecavelier Des Etangs (2006) were able to detect multiple transits of HD 189733b, leading to a significant improvement in the determination of its period. *Hipparcos* photometry has therefore been demonstrated to be precise enough to detect the transit of a Hot Jupiter around stars that are fainter than HD 168443 ( $V=6.92$ ). The top panels of Figure 3 show the *Hipparcos* photometry of HD 209458 plotted against Julian Date and also against orbital phase of the star’s Hot-Jupiter companion. A few observations fall within the modern transit window and show a clear dimming. The bottom two panels are similar plots for HD 168443. Using our new radial velocity observations, we followed the prescription of Robichon & Arenou (2000) to create the phased plot with the predicted transit set at zero phase. Three *Hipparcos* photometric observations acquired around BJD 2448050 lie inside of our predicted transit window. Unlike the case for HD 209458, the *Hipparcos* photometry show no evidence for a transit. However, the expected transit depth for HD 168443b is significantly smaller than HD 209458; the *Hipparcos* photometry alone would have been an unreliable guide to prove or disprove the occurrence of transits in HD 168443. Nevertheless, we advocate such a check for bright stars with sufficiently precise orbital ephemerides.

## 7. Photometry of the Revised Transit Window

In addition to the new TERMS photometry presented below, we also observed HD 168443 with the Southeastern Association for Research in Astronomy (SARA) 0.6 m telescope at Cerro Tololo Inter-American Observatory. However, due to poor weather conditions, the SARA-S measurements exhibited scatter that was significantly higher than the predicted transit depth. Therefore, we do not discuss these data further, but we note that planning such multi-site observations is necessary in our TERMS search for long-period transits.

### 7.1. Cerro Tololo Inter-American Observatory (CTIO)

Before we had access to the latest Keck-HIRES radial velocities, we used published orbital parameters (Wright et al. 2009) to calculate the transit ephemeris and to schedule an observing run for 2010 September 7 with the CTIO 1.0 m telescope and Y4KCam CCD detector. The observations were made through a Johnson-Morgan R-band filter; instrumental magnitudes of HD 168443 and comparison stars were extracted from the images with an IDL implementation of DAOPHOT (Stetson P. 1987). Relative fluxes (Everett & Howell 2001) of HD 168443 were computed with respect to the two stable comparison stars (TYC 5681-1450-1 and TYC 5681-1458-1).

The results are plotted in Figure 4. The solid curve represents the predicted transit fluxes computed from our new orbital elements in Table 2, assuming on-time, central transits with a predicted depth of 0.6% or 0.006 flux units. The scatter of the measurements is 0.0027, easily sufficient to detect the predicted transits. However, these measurements cover only the later part of the predicted transit window; an egress late by  $1\sigma$  and  $3\sigma$  are represented with dashed blue and red lines, respectively. The CTIO data show only that late transits do not occur.

We have presented these measurements because CTIO photometric monitoring is an essential component of the TERMS strategy. Had the ephemerides (based on orbital parameters in the literature) been more precise, the CTIO photometry has the requisite precision to detect a predicted on-time transit. Our results demonstrate the precision achievable from CTIO with a typical TERMS target.

### 7.2. Fairborn Observatory

We obtained additional photometric observations of HD 168443 with the T8 0.8 m automatic photometric telescope (APT) at Fairborn Observatory in southern Arizona. The T8 APT uses a two-channel precision photometer with two EMI 9124QB bi-alkali photomultiplier tubes to make simultaneous measurements in the Strömgren  $b$  and  $y$  passbands. The telescope was programmed to make nightly differential brightness measurements of HD 168443 with respect to the comparison star HD 166664. Three consecutive differential measurements were co-added to create a single nightly differential magnitude. To improve the precision of these brightness measurements, we combined the individual  $b$  and  $y$  differential magnitudes into a mean  $(b + y)/2$  "passband". The typical precision of a single observation on good nights is  $\sim 0.0015$  mag. See (Henry 1999) for further details on telescope design and operations, data reduction, calibrations, and data precision.



Between 2011 March 2 and June 19, the APT collected 107 nightly observations of HD 168443 with respect to HD 166664; the differential  $(b + y)/2$  magnitudes were converted to relative fluxes and are plotted in Figure 5. The nightly observations scatter about their mean flux, indicated by the dashed line in Figure 5, with a standard deviation of 0.0016, which is consistent with constant stars. Periodogram analyses from one to 100 days reveal no significant periodicity. We conclude that HD 168443 is constant on its rotation timescale. A least-squares sine fit of the nightly observations on the orbital period of 168443b gives a semi-amplitude of  $0.00026 \pm 0.00023$  flux units. This very low limit to brightness variability in HD 168443 on the 58-day orbital period indicates that rotational modulation of starspots is not the cause of the radial velocity variations, see e.g., (Queloz et al. 2001).

We also used the T8 APT to monitor HD 168443 on two nights in the 2011 observing season when our new ephemeris predicted additional transit events. Each monitoring observation consists of a single differential measurement rather than the mean of three observations, as we used for the nightly observations; thus the monitoring observations will have more scatter than the nightly observations.

On 2011 April 28 UT, an observable egress was to occur at BJD 2,455,679.937. We successfully monitored the star and obtained the 80 measurements plotted in Figure 6. The star was still two months before its opposition, so the start time was delayed until the star rose above an airmass of  $\sim 2.0$ ; the observations ended 3.3 hours later (at dawn). The sudden increase of the scatter after predicted egress is the result of a plume of smoke from one of the many wildfires burning throughout southern Arizona at the time. The standard deviation of the entire data set is 0.0040 flux units. The solid curve in Figure 6 represents the predicted fluxes for an on-time, central transit. The dotted blue lines represent the  $\pm 1\sigma$  uncertainty in the predicted time of central transit. The difference between the mean flux of the 47 pre-egress observations and the 33 post-egress observations is only  $0.0005 \pm 0.0011$ . Given the tight limit on the transit time (35 min or 0.024 day), these observations rule out central transits with the predicted depth of 0.006 with a SNR of  $\sim 5 : 1$ .

The next predicted transit was calculated to occur 58 days later on 2011 June 25 UT, centered at BJD 2,455,737.862. HD 168443 was at opposition during this transit, so we were able to acquire 165 observations over an interval of 7.1 hours. The declination of HD 168443 is approximately  $-10^\circ$ , so the airmass values at the start and at the end of the night were 2.25 and 2.51, respectively, for the the east and west observing limits. Atmospheric extinction was also significantly higher than normal at the beginning of the night due to airborne dust, which gradually settled out over the course of the night. Therefore, in addition to reducing the transit observations with larger than normal extinction coefficients, we also removed a linear trend of approximately 0.008 flux units via a linear least-squares fit. The residuals

from the line fit are plotted in Figure 7, again compared with predicted transit fluxes. The overall scatter of the 165 observations is 0.0039 flux units.

Finally, we estimate an upper limit to the possible transits of HD 168443b. The mean *differential magnitudes* of the T8 nightly observations in Figure 5 and of the mean of the first and second T8 transit monitoring observations in Figures 6 & 7, before they were converted to relative fluxes, are  $-0.24041 \pm 0.00017$  mag,  $-0.23961 \pm 0.00050$  mag, and  $-0.24044 \pm 0.00037$  mag, respectively. So, the observed difference between the mean of the nightly observations and the mean of the transit observations is only  $0.00038 \pm 0.00045$  mag or  $0.00035 \pm 0.00041$  flux units. Therefore, we should have been able to detect a transit depth of 0.2% or 0.002 at a SNR of almost 5:1, but our observations show no evidence of a transit.

### 7.3. Full Coverage of the Transit Window

The entire transit window was covered during the three monitoring nights. Initially, we were able to rule out only a late egress using 1-meter CTIO photometry from 2010 September 8 with  $(3-\sigma)$  confidence. We further confirmed this result with the APT photometry on June 25 by ruling out a late ingress  $(3-\sigma)$ . The early  $(1-\sigma)$  and on time egress was ruled out with APT photometry from April 28, 201. In Figure 8 we present a phase plot containing all three monitoring nights. Since both data sets from the T8 APT used the same reference star, we placed the median of the measurements on the same y-axis scale. The CTIO data set was adjusted with an offset using the overlapping points from CTIO and the APT. The center of predicted transit is at phase 0.0, marked by a solid vertical line. The dotted blue lines represent  $1-\sigma$  early and late windows while the dashed red lines represent  $3-\sigma$  deviation from the center of the predicted transit.

## 8. Discussion

As part of our ongoing Transit Ephemeris Refinement and Monitoring Survey (TERMS), we present revised orbital parameters for the HD 168443 system, based on 130 radial velocity measurements with Keck-HIRES that span almost 15 years. Using the transit ephemerides derived from the revised orbital parameters, we searched for a transit using telescopes from CTIO, Fairborn Observatory, and SARA-S. We find no evidence of a detectable transit. The presence of a non-grazing transit corresponding to our model ( $1.1R_J$  planet) is ruled out at a high level of confidence with high precision photometry acquired by the APT. Grazing transits or transits with a planet radii as small as  $0.58 R_{Jup}$  (which would yield densities

much too high) are formally excluded at  $1\text{-}\sigma$  confidence, though the smaller duration of such transits implies that the time of our photometric observations could have missed the ingress and egress. Using our orbital solution, and the planetary and stellar radii presented in this paper, we derive an upper limit on inclination of the system at  $87.8^\circ$  using methods described by Kane & von Braun (2008).

Even with a number of RV observations, determining precise orbital parameters for one component of a multi-planet system can be difficult. The recent discovery of transits of 55 Cnc e by (Winn et al. 2011), based on a new orbital period by Dawson & Fabrycky (2010), illustrates the insidious impact of aliases and harmonics. Nevertheless, these effects can be mitigated by careful observation and analysis, and the value of additional precision radial velocities and revised orbital parameters cannot be overstated.

While we do not see transits in the HD 168443 system, the experimental approach outlined here, combining high precision radial velocity with multiple photometric telescope facilities, is worth pursuing in the quest for new transiting planets around bright nearby stars.

### Acknowledgements

This work made use of the SIMBAD database (operated at CDS, Strasbourg, France), NASA’s Astrophysics Data System Bibliographic Services, and the NASA Star and Exoplanet Database (NStED). This work was partially supported by funding from the Center for Exoplanets and Habitable Worlds, supported by the Pennsylvania State University, the Eberly College of Science, and the Pennsylvania Space Grant Consortium. The authors would also like to thank Andrés Jordán for providing support for the observations at CTIO. G.W.H. acknowledges support from NASA, NSF, Tennessee State University, and the Tennessee Centers of Excellence Program. ELNJ acknowledges support from NSF grant AST-0721386. M.R. acknowledges support from ALMA-CONICYT projects 31090015 and 31080021. We would also like to thank the referee for insightful comments that helped us to improve this paper. Finally, the authors wish to extend special thanks to those of Hawai‘ian ancestry on whose sacred mountain of Mauna Kea we are privileged to be guests. Without their generous hospitality, the Keck observations presented herein would not have been possible.

## REFERENCES

- Bakos, G., Noyes, R.W., Kovacs, G., Stanek, K.Z., Sasselov, D.D. & Domsa, I., 2004, *PASP*, 116, 266
- Barbieri, M., et al. 2007, *A&A*, 476, L13
- Barge, P., et al., 2008, *A&A*, 482, L17
- Bessell, M. S., 2000, *PASP*, 112, 961
- Bodenheimer, P., Laughlin, G., Lin, D.N.C., 2003, *ApJ*, 592, 555
- Borucki, W. J., et al. 2011, *ApJ*, 728, 117
- Bouchy, F., et al. 2005, *A&A*, 444, L15
- Butler, R.P., Marcy, G.W., Williams, E., McCarthy, C., Dosanji, P., Vogt, S.S., 1996, *PASP*, 108, 500
- Castellano, T., Jenkins, J., Trilling, D. E., Doyle, L., & Koch, D. 2000, *ApJ*, 532, L51
- Charbonneau, D., Brown, T. M., Latham, D. W., & Mayor, M. 2000, *ApJ*, 529, L45
- Colon, K. D., Ford, E. B., Redfield, S., Fortney, J. J., Shabram, M., Deeg, H. J., & Mahadevan, S. 2010, *MNRAS*, submitted
- Dawson, R. I., & Fabrycky, D. C. 2010, *ApJ*, 722, 937
- Demarque, P., Woo., J., Kim, Y., Yi, S.K., 2004, *ApJS*, 155, 667
- Eastman, J., Siverd, R., & Gaudi, B. S. 2010, *PASP*, 122, 935
- Everett, M.E., Howell, S.B., 2001, *PASP*, 113, 1428
- Fossey, S. J., Waldmann, I. P., & Kipping, D. M. 2009, *MNRAS*, 396, L16
- Hébrard, G., & Lecavelier Des Etangs, A. 2006, *A&A*, 445, 341
- Henry, G. W. 1999, *PASP*, 111, 845
- Henry, G. W., Marcy, G. W., Butler, R. P., & Vogt, S. S. 2000, *ApJ*, 529, L41
- Henry, G. W., Howard, A. W., Marcy, G. W., Fischer D. A., Johnson, J. A., 2011, *ApJ*, Submitted

- Howard, A.W., et al., 2009, ApJ, 696, 75
- Howard, A.W., et al., 2010, ApJ, 721, 1467
- Isaacson, H., Fischer, D.A., 2010, ApJ, 725, 875
- Kane, S.R., von Braun, K., 2008, ApJ, 689, 492
- Kane, S. R., Mahadevan, S., von Braun, K., Laughlin, G., & Ciardi, D. R. 2009, PASP, 121, 1386
- Kane, S. R., Howard, A. W., Pilyavsky, G., Mahadevan, S., Henry, G. W., von Braun, K., Ciardi, D. R., Dragomir, D., Fischer, D. A., Jensen, E., Laughlin, G., Ramirez, S. V., Wright, J. T., 2011, ApJ, 733, 1
- Marcy, G. W., Butler, R. P., Vogt, S. S., Fischer, D., & Liu, M. C. 1999, ApJ, 520, 239
- Marcy, G. W., et al. 2001, ApJ, 555, 418
- Marcy, G.W., Butler, R.P., Vogt, S.S., Fischer, D.A., Henry, G.W., Laughlin, G., Wright, J.T., Johnson, J.A., 2005, ApJ, 619, 570
- Marcy, G.W., Butler, R.P., 1992, PASP, 104, 270
- McCullough, P. R., Stys, J. E., Valenti, J. A., Fleming, S. W., Janes, K. A., & Heasley, J. N. 2005, PASP, 117, 783
- Moutou, C., et al. 2009, A&A, 498, L5
- Pollacco, D.L., et al., 2006, PASP, 118, 1407
- Perryman, M. A. C., & Schulze-Hartung, T. 2011, A&A, 525, A65
- Queloz, D., Henry, G. W., Sivan, J. P., Baliunas, S. L., Beuzit, J. L., Donahue, R. A., Mayor, M., Naef, D., Perrier, C., and Udry, S. 2001, A&A, 379, 279
- Redfield, S., Endl, M., Cochran, W. D., & Koesterke, L. 2008, ApJ, 673, L87
- Reffert, S., & Quirrenbach, A. 2011, A&A, 527, A140
- Reffert, S., & Quirrenbach, A. 2006, A&A, 449, 699
- Robichon, N., & Arenou, F. 2000, A&A, 355, 295
- Sahlmann, J., et al. 2011, A&A, 525, A95

- Sato, B., et al. 2005, *ApJ*, 633, 465
- Sing, D. K., et al. 2011, *A&A*, 527, A73
- Snellen, I. A. G., Albrecht, S., de Mooij, E. J. W., & Le Poole, R. S. 2008, *A&A*, 487, 357
- Stetson, P. B. 1987, *PASP*, 99, 191
- Udry, S., Mayor, M., Naef, D., Pepe, F., Queloz, D., Santos, N. C., & Burnet, M. 2002, *A&A*, 390, 267
- Valenti, J.A., Butler, R.P., Marcy, G.W., 1995, *PASP*, 107, 966
- Valenti, J.A., Piskunov, N., 1996, *A&AS*, 118, 595
- Valenti, J.A., Fischer, D.A., 2005, *ApJS*, 159, 141
- Valenti, J.A., et al., 2009, *ApJ*, 702, 989
- van Belle, G. T., & von Braun, K. 2009, *ApJ*, 694, 1085
- van Leeuwen, F., 2007, *A&A*, 474, 653
- Veras, D., & Armitage, P. J. 2007, *ApJ*, 661, 1311
- Veras, D., & Ford, E. B. 2010, *ApJ*, 715, 803
- Vidal-Madjar, A., et al. 2011, *A&A*, 527, A110
- Vogt, S.S., et al., 1994, *Proc. SPIE*, 2198, 362
- von Braun, K., Kane, S.R., Ciardi, D.R., 2009, *ApJ*, 702, 779-790
- Winn, J.N., et al., 2011, *ApJ Letters*, 737, 1, L18
- Wright, J.T., 2005, *PASP*, 117, 657
- Wright, J. T., Upadhyay, S., Marcy, G. W., Fischer, D. A., Ford, E. B., & Johnson, J. A. 2009, *ApJ*, 693, 1084
- Wright, J.T., Howard, A.W., 2009, *ApJS*, 182, 205

Table 1. Stellar Properties

Parameter	Value	Reference
$M_V$	4.198	van Leeuwen (2007)
$B - V$	0.724	Bessell (2000)
$V$	6.92	Bessell (2000)
Distance (pc)	$37.4 \pm 1.0$	van Leeuwen (2007)
$T_{\text{eff}}$ (K)	$5491 \pm 44$	This work
$\log g$	$4.07 \pm 0.06$	This work
[Fe/H]	$+0.04 \pm 0.03$	This work
$v \sin i$ (km s $^{-1}$ )	$2.20 \pm 0.50$	This work
$M_{\star}$ ( $M_{\odot}$ )	$0.995 \pm 0.019$	This work
$R_{\star}$ ( $R_{\odot}$ )	$1.51 \pm 0.06$	This work
$\log R'_{\text{HK}}$	$-5.088$	This work
$S_{\text{HK}}$	0.148	This work

Table 2. Keck Radial Velocities

BJD – 2440000	Radial Velocity ( $\text{m s}^{-1}$ )	Uncertainty ( $\text{m s}^{-1}$ )
10276.90890	-309.29	1.73
10603.01184	-33.47	1.02
10665.86781	-69.33	1.24
10713.73770	-73.02	1.14
10714.76649	-71.38	1.13
10955.01039	-5.57	1.12
10955.95862	-5.13	1.02
10957.07105	-4.68	1.05
10981.88012	-568.69	1.01
10982.89132	-492.38	1.10
10983.07690	-472.56	1.10
10983.82231	-420.40	1.16
10984.06138	-407.63	1.14
11009.87009	22.04	1.34
11010.05994	24.94	0.93
11010.85123	20.67	1.17
11011.86077	25.19	1.37
11012.95413	19.19	1.14
11013.06816	20.31	0.82
11013.82791	15.69	1.15
11013.92983	15.33	1.20
11042.95557	-326.88	1.09
11043.95602	-276.32	1.19
11050.81406	-77.68	1.26
11068.77042	54.21	1.08
11069.78596	60.86	1.09
11070.79807	52.81	1.09
11071.76998	50.98	1.11
11072.76271	47.77	1.26
11074.78514	39.07	1.09
11228.16111	91.81	1.07
11229.14942	95.62	1.32
11311.04174	151.35	1.27
11312.07757	137.66	1.23
11313.07589	124.69	1.18
11314.08699	103.43	1.20



Table 2—Continued

BJD – 2440000	Radial Velocity ( $\text{m s}^{-1}$ )	Uncertainty ( $\text{m s}^{-1}$ )
11341.02661	109.66	1.11
11341.90588	129.71	1.03
11342.97144	142.29	1.20
11367.86065	214.31	1.30
11368.84314	205.20	1.40
11370.01150	188.83	1.14
11370.91933	171.14	0.73
11371.91024	153.12	1.11
11372.87811	131.18	1.16
11373.79496	105.31	1.44
11409.85005	276.28	1.14
11410.84584	278.53	1.29
11411.84641	288.70	1.21
11438.73808	-282.82	1.19
11439.73057	-414.58	1.18
11440.71830	-527.69	1.22
11441.73997	-616.71	1.20
11679.04801	-109.80	1.09
11680.07181	-20.27	1.29
11703.01759	488.68	1.19
11703.98840	488.90	1.17
11705.03899	493.45	1.27
11705.95846	499.46	1.30
11707.08125	502.77	1.20
11754.85883	473.14	1.66
11755.90986	489.51	1.06
11792.74760	-338.38	1.01
11793.80008	-223.10	1.25
11882.68333	496.02	0.88
11883.68272	498.30	0.86
11983.15885	333.08	1.01
11984.15396	335.98	1.35
12004.12317	357.01	1.33
12005.14737	352.21	1.37
12007.13381	329.80	1.16
12008.03597	311.14	1.37

Table 2—Continued

BJD – 2440000	Radial Velocity ( $\text{m s}^{-1}$ )	Uncertainty ( $\text{m s}^{-1}$ )
12009.10491	294.16	1.24
12030.98196	-27.97	1.26
12061.94969	278.32	1.37
12062.96034	259.31	1.54
12094.88634	78.37	1.40
12096.93360	110.11	1.52
12098.01419	126.96	1.38
12099.02269	145.64	1.34
12099.93319	147.47	1.23
12100.94388	158.52	1.41
12101.88510	171.72	1.42
12127.86347	57.89	1.51
12128.79403	30.56	1.23
12133.78671	-210.61	1.53
12160.80699	79.11	1.48
12189.76875	-156.78	1.43
12445.93556	-192.60	1.38
12486.81165	-930.27	1.38
12515.75755	-85.29	1.44
12536.74799	-258.80	1.39
12572.69122	-74.58	1.31
12713.14689	-280.58	1.33
12778.02605	-891.12	1.36
12804.06082	12.02	1.25
12834.88152	-730.70	1.31
12848.80396	-133.69	1.29
12855.96590	0.22	1.28
12898.71740	-579.54	1.16
13154.04176	260.17	1.49
13180.90222	-183.23	1.37
13195.84965	58.60	1.13
13238.88150	-123.80	1.17
13301.73743	-565.16	1.16
13546.89064	334.18	1.14
13842.12630	125.12	1.18
13927.87788	-3.76	1.15

Table 2—Continued

BJD – 2440000	Radial Velocity (m s <sup>-1</sup> )	Uncertainty (m s <sup>-1</sup> )
13984.83683	-51.21	0.96
14314.99539	-101.88	1.26
14335.95562	-191.79	1.23
14343.88345	-620.98	1.00
14344.94159	-744.93	1.11
14398.74642	-344.38	1.08
14546.11545	-16.53	1.17
14548.15404	10.39	1.27
14720.84072	102.86	1.11
14956.12833	289.18	1.53
14985.11014	-473.97	1.33
15014.97707	332.37	1.13
15026.96186	318.51	1.22
15106.74809	-279.16	1.20
15286.11499	173.04	1.21
15322.08481	403.90	1.21
15343.00253	103.85	1.36
15374.84199	453.14	1.16
15378.82083	413.14	1.21
15403.81739	198.38	1.22
15490.73506	346.47	1.30
15636.13540	-128.87	1.05

Table 3. Keplerian Orbital Model

Parameter	Value
HD 168443 b	
$P$ (days)	$58.11247 \pm 0.0003$
$T_c^a$ (JD – 2,440,000)	$15621.637 \pm 0.0156$
$T_p^b$ (JD – 2,440,000)	$15626.199 \pm 0.024$
$e$	$0.52883 \pm 0.00103$
$K$ (m s $^{-1}$ )	$475.133 \pm 0.9102$
$\omega$ (deg)	$172.923 \pm 0.139$
$M \sin i$ ( $M_{\text{Jup}}$ )	$7.659 \pm 0.0975$
$a$ (AU)	$0.2931 \pm 0.00181$
HD 168443 c	
$P$ (days)	$1749.83 \pm 0.57$
$T_c^a$ (JD – 2,440,000)	$15599.9 \pm 1.187$
$T_p^b$ (JD – 2,440,000)	$15521.3 \pm 2.2$
$e$	$0.2113 \pm 0.00171$
$K$ (m s $^{-1}$ )	$297.70 \pm 0.618$
$\omega$ (deg)	$64.87 \pm 0.5113$
$M \sin i$ ( $M_{\text{Jup}}$ )	$17.193 \pm 0.21$
$a$ (AU)	$2.8373 \pm 0.018$
System Properties	
$\gamma$ (m s $^{-1}$ )	$-46.533 \pm 0.552$
$dv/dt$ (m s $^{-1}$ yr $^{-1}$ )	$-0.00868 \pm 0.00025$
Measurements and Model	
$N_{\text{obs}}$	130
rms (m s $^{-1}$ )	3.90
$\chi^2_\nu$	1.44

<sup>a</sup>Time of transit.

<sup>b</sup>Time of periastron passage.

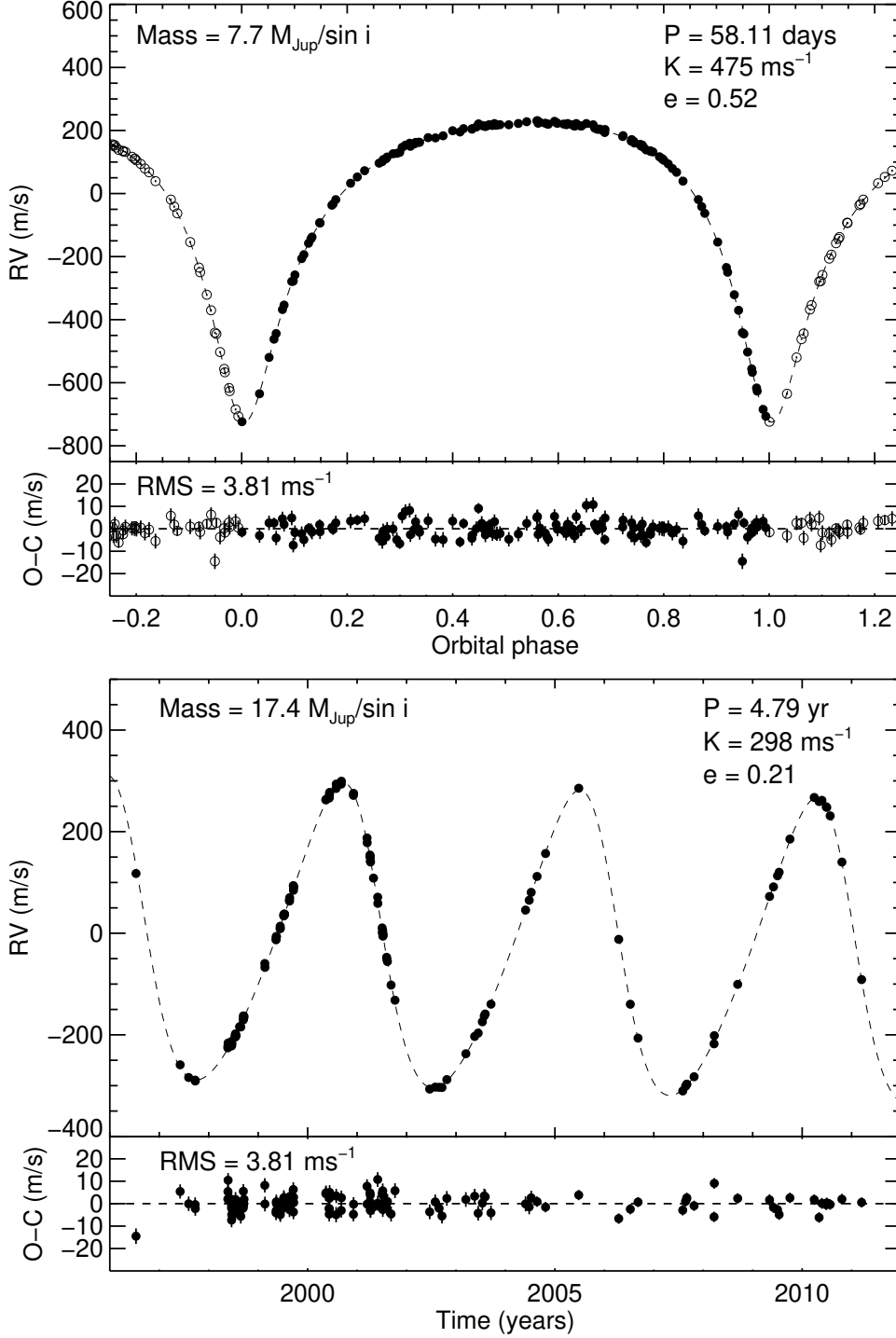


Fig. 1.— RV measurements of HD 168443 from Keck-HIRES (filled circles) with Keplerian orbital model (dashed lines). The top panel shows the RVs phased to the orbital period of HD 168443 b with the model for the other planet and linear trend subtracted. Open circles represent the same RV measurements wrapped one orbital phase. The bottom panel shows the RV time series illustrating the variations due to HD 168443 c, with the linear velocity trend and the orbit of HD 168443 b subtracted.

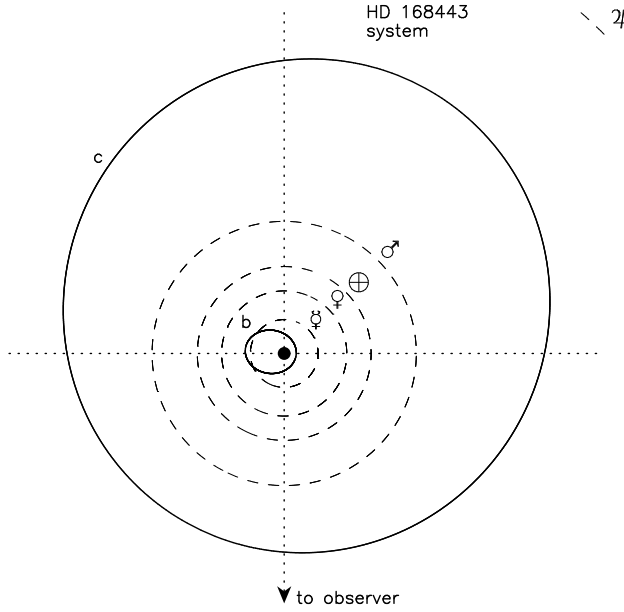


Fig. 2.— The orbits of the planets HD 168443b and HD 168443c shown in solid lines. Orbits of Mercury (eccentricity set to zero for clarity) through Jupiter are represented with dashed ovals.

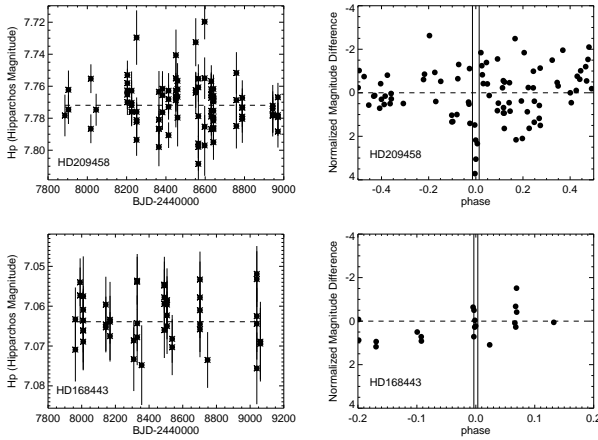


Fig. 3.— *Hipparcos* Photometry. Top left: Photometric measurements of HD 209458 over the course of three years. Top right: the same data plotted vs. orbital phase, with the transit corresponding to zero phase. The transit is clearly visible and is marked by two vertical lines. Bottom left: *Hipparcos* Photometric measurements of HD 168443 taken over the course of three years. Bottom right: Similar to the plot for HD 209458 (following the method of Robichon & Arenou (2000)). The predicted window is bounded by two vertical lines, with three *Hipparcos* measurements obtained during the predicted transit. No transit is evident.

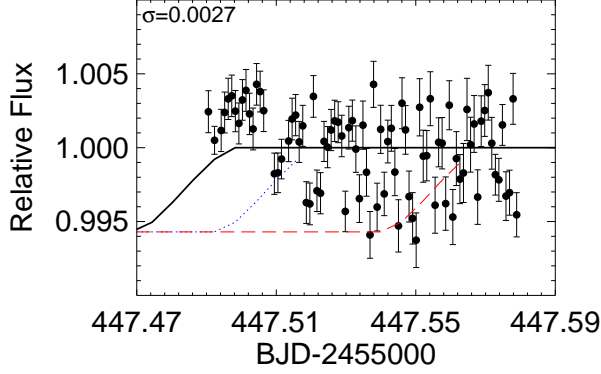


Fig. 4.— Relative photometry from CTIO. The standard deviation of 0.0027 in the normalised flux is precise enough to detect the predicted transit, which would cause a 0.006 decrease. The solid line represents the predicted transit after ephemeris refinement using Keck HIReS data, with the predicted egress occurring right before the measurements were acquired. The dotted blue and the dashed red lines represent the  $1\text{-}\sigma$  and  $3\text{-}\sigma$  uncertainties in the time of egress.

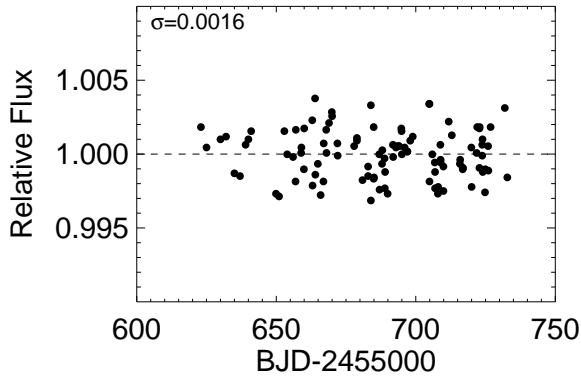


Fig. 5.— Photometry from the T8 APT consisting of 107 measurements over the span of 109 days. The dashed line represents the normalised flux. The standard deviation from the mean is 0.0016.

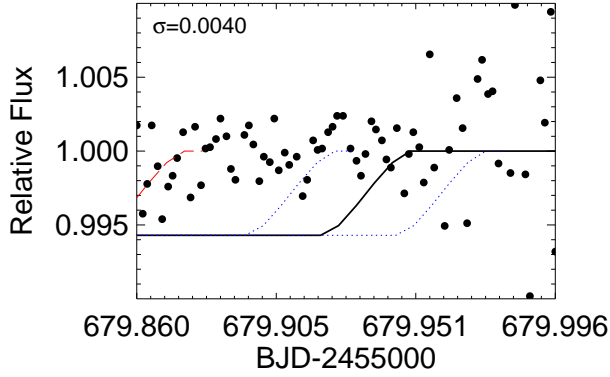


Fig. 6.— Photometric observations of HD 168443 acquired with the T8 APT at Fairborn Observatory during the predicted transit of 2011 April 28. The standard deviation of 0.0040 flux units is sufficient to detect the predicted transit egress (solid line) if present. The dotted blue lines represent the  $\pm 1 - \sigma$  uncertainty in the transit time. There is no evidence for an egress event.

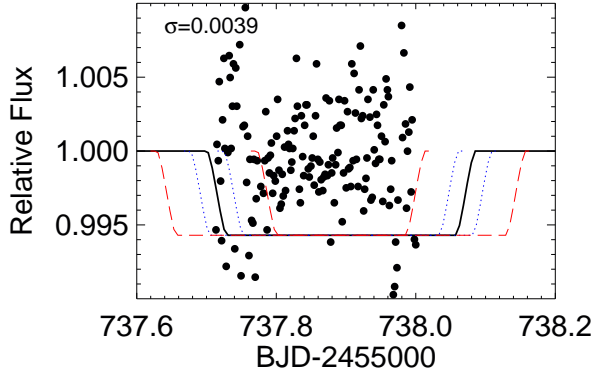


Fig. 7.— Photometric observations of HD 168443 with the T8 APT during the predicted transit of 2011 June 25. The standard deviation of 0.0039 flux units is sufficient to detect the predicted transit egress (solid line) if present. The dotted blue lines represent the  $\pm 1 - \sigma$  uncertainty in the transit time. Again, there is no indication of a transit.



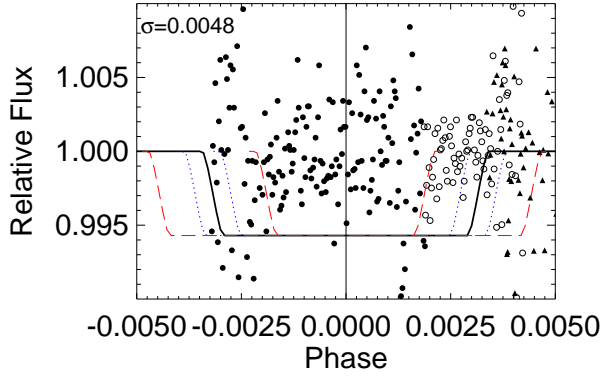


Fig. 8.— Phase diagram of the observations from all three nights of transit monitoring. The filled and unfilled circles are the T8 APT measurements from 2011 June 25 and April 28, respectively. The filled triangles are the CTIO observations from 2010 September 7. As in earlier figures, the solid line represents the predicted flux changes during a transit. The dotted blue and the dashed red lines represent  $\pm 1 - \sigma$  and  $\pm 3 - \sigma$  deviations in the time of transit, respectively.